Radiotherapy and Oncology 134 (2019) 135–142

Contents lists available at ScienceDirect

Radiotherapy and Oncology

journal homepage: www.thegreenjournal.com

Original Article

The dosimetric effect of residual breath-hold motion in pencil beam scanned proton therapy – An experimental study

Jenny Gorgisyan [a,b,c,1,*], Antony J. Lomax [a,d], Per Munck af Rosenschold [c,e], Gitte F. Persson [b,2], Miriam Krieger [a,d], Emma Colvill [a], Jonas Scherman [e], Francis Gagnon-Moisan [a], Martina Egloff [a], Giovanni Fattori [a], Svend Aage Engelholm [b], Damien C. Weber [a,f], Rosalind Perrin [a,3]

[a] Paul Scherrer Institute, ETH Domain, Switzerland; [b] Department of Oncology, Rigshospitalet Copenhagen University Hospital; [c] Niels Bohr Institute, University of Copenhagen, Denmark; [d] Department of Physics, ETH Zürich, Switzerland; [e] Radiation Physics, Department of Hematology, Oncology and Radiation Physics, Skåne University Hospital, Sweden; [f] Radiation Oncology Department, University Hospital of Zürich, Switzerland

ARTICLE INFO

Article history:
Received 20 October 2017
Received in revised form 25 January 2019
Accepted 27 January 2019
Available online 14 February 2019

Keywords:
4D phantom
PBS proton therapy
Breath-hold
Lung tumours

ABSTRACT

Background and purpose: Motion management in the treatment of lung cancer is necessary to assure highest quality of the delivered radiation therapy. In this study, the breath-hold technique is experimentally investigated for pencil beam scanned (PBS) proton therapy, with respect to the dosimetric effect of residual breath-hold motion.

Material and methods: Three-dimensional (3D)-printed tumours extracted from CT scans of three patients were inserted into a dynamic anthropomorphic breathing phantom. The target was set up to move with the individual patient's tumour motion during breath-hold as previously assessed on fluoroscopy. Target dose was measured with radio-chromic film, and both single field uniform dose (SFUD) and intensity-modulated proton therapy (IMPT) plans were delivered. Experiments were repeated for each patient without any motion, to compute the relative dose deviation between static and breath-hold cases.

Results: SFUD plans showed small dose deviations between static and breath-hold cases, as evidenced by the gamma pass rate (3%, 3 mm) of 85% or higher. Dose deviation was more evident for IMPT plans, with gamma pass rate reduced to 50–70%.

Conclusions: The breath-hold technique is robust to residual intra-breath-hold motion for SFUD treatment plans, based on our experimental study. IMPT was less robust with larger detected dose deviations.
 Radiotherapy and Oncology 134 (2019) 135–142

Motion management in pencil beam scanned (PBS) proton therapy of mobile lung tumours is a prerequisite for accurate dose delivery [1]. Due to uncertainties caused by the motion (e.g. [2]), only a few PBS proton therapy centres offer lung cancer treatments [3], despite PBS potentially being superior to other techniques [4]. It should be mentioned however, that many lung cancer patients have been treated by ion beam therapy with good results (e.g. [5]). Similarly to conventional treatments with photons, for proton treatments, motion is typically accounted for in the planning step by increasing the margins around the target. This is often done on a patient specific basis [1,6], with the internal target volume (ITV) based on, for example, maximum-intensity-projections (MIP) of four dimensional CT (4DCT) phases [7]. The use of range-adaptive margins for PBS treatments of moving targets has also been proposed, whereby the water-equivalent path length changes of the planned pencil beams over the respiratory cycle are taken into account [8,9]. A disadvantage of the ITV method however, is the dose to the non-tumour tissue contained within the ITV. An alternative approach could be robust treatment planning, where plans are optimised to be robust to setup and range uncertainties [10], which can also be extended to include motion. This approach however has been shown to be extremely sensitive to changes in motion pattern over the course of treatment [11,12]. For small motions (<5 mm), rescanning is efficient in minimizing the interplay effect [9,13]. For larger motion, beam gating [14] and breath-hold [15] can substantially decrease the motion effect on the dosimetry. For the latter techniques, the target volume is decreased as compared to the ITV-concept, and thereby also the dose to the surrounding OARs, but at the expense of increased

* Corresponding author at: CHUV – Institut de Radiophysique, Rue du Grand-Pré 1, 1007 Lausanne, Switzerland.
E-mail address: jenny.gorgisyan@chuv.ch (J. Gorgisyan).
[1] Current affiliation: Institute of Radiation Physics, Lausanne University Hospital, Lausanne, Switzerland.
[2] Current affiliation: Department of Oncology, Herlev Hospital, University of Copenhagen, Herlev, Denmark and Department of Clinical Medicine, Faculty of Medical Science, University of Copenhagen, Herlev, Denmark.
[3] Current affiliation: Universitätsklinikum Erlangen, Department of Medical Radiation Physics, Strahlenklinik, Universitätsstr, 29, 91054 Erlangen, Germany.

https://doi.org/10.1016/j.radonc.2019.01.033
0167-8140/

treatment duration [8,16]. Lastly, tumour tracking may provide the optimal solution to the motion problem in scanned ion beams, but it is difficult to realise due to high requirements of both online imaging and fast feedback for beam adaptation [12].

The breath-hold technique has been explored extensively for photon radiotherapy with promising results [17,18]. For proton therapy, the dosimetric effect of the difference in tumour position from breath-hold to breath-hold (inter-breath-hold motion) has been shown to be acceptable [15,19]. Positional variations occurring during the breath-hold (intra-breath-hold motion) on the other hand, may cause interference patterns with the motion of the treatment delivery (interplay effect) [20,21], and should be investigated.

Previous investigations of breath-hold treatment in PBS proton therapy are so far only simulation studies. There is however no clinically relevant experimental evidence currently to support these simulations.

Regardless of the motion management technique, imaging of the tumour (including the motion) prior to the treatment is necessary. In addition to 4DCT scans, tumour motion can be evaluated with fluoroscopy that generally has higher time resolution. Lung tumours can be difficult to visualise using this image modality however, especially if the tumour is close to, or within, soft tissue. Different types of implanted markers have been applied to increase the visibility of the tumour, e.g. metal [22] or liquid fiducials [23,24]. Further, the motion information from fluoroscopy is typically limited to 2D-data. By combining motion patterns from fluoroscopy with 4DCT scans, a more comprehensive analysis of the motion, and the effects thereof, could be performed [16,25]. Another use of the fluoroscopy data is to use the motion pattern as input into a phantom, e.g. an anthropomorphic phantom [26,27].

The aim of this study was to investigate the dosimetric effect of intra-breath-hold target motion measured in the target of a dynamic anthropomorphic breathing phantom. We investigated this dosimetric effect on individual patient's three-dimensional (3D)-printed lung tumours and motion patterns from fluoroscopic examinations. Both single field uniform dose (SFUD) and intensity-modulated proton therapy (IMPT) [28] plans were delivered. To the author's knowledge, this is the first study to experimentally measure the possible dose degradation caused by residual intra-breath-hold motion in PBS proton therapy under realistic clinical conditions.

Methods and materials

Image data

Imaging studies from three patients (breath-hold CT and fluoroscopy) were selected from a cohort of fifteen patients with locally-advanced non-small cell lung cancer, enrolled on a prospective radiotherapy trial at the Rigshospitalet, Denmark [29]. The three patients had been injected with a liquid fiducial marker BioXMark® (Nanovi Radiotherapy A/S Lyngby, DK) in or near the primary tumour. The patients had undergone extra image sessions including fluoroscopy taken both in free-breathing (20 seconds) and in breath-hold (2 × 10–15 s) at days 2, 16 and 31 of the treatment course. They were subsequently enrolled in this proton therapy phantom study at the Paul Scherrer Institute (PSI).

Phantom

The in-house-developed dynamic anthropomorphic breathing phantom, Lung Cancer (LuCa), has been thoroughly investigated regarding physical characteristics and motion reproducibility by Perrin et al. [27]. The phantom consists of an artificial lung that can be inflated by a ventilation system (Fig. 1). A cylinder embedded in the lung (ϕ70 mm) contains the target, and can be accessed from the inferior end of the phantom. By changing the lung pressure, the cylinder containing the target moves in the superior-inferior direction, with its actual displacement being detected by an optical distance sensor.

Targets

The target structures were extracted from the Eclipse treatment planning system (Varian Medical Systems, Palo Alto, CA, USA). The targets were scaled to fit the cylinder tube in the phantom and then 3D-printed (Fig. 2), with the orientation of the target optimised such that a scaling factor as small as possible was used. Targets (VisiJet M3 Crystal) and cylindrical holders (Acrylnitril-Butadien-Styrol (ABS) with a honey-comb pattern to simulate lung tissue) were printed using ProJet© 3500 SD&HD 3D-printer (3D Systems GmbH, Darmstadt, DE) and Dimension Elite 3D-printer (Stratasys, Eden Prairie, MN, USA), respectively (Fig. 2). Radiochromic films were inserted in the coronal planes for patient 1, and transversal planes for patients 2 and 3. The relative proton stopping power to water (RPSW) of the tumour and the holder materials were measured to be 1.15 and 0.15, respectively, as shown together with other material properties in Supplementary Table S1. In addition to these targets, a spherical wooden target (ϕ60 mm, films in coronal planes) was also used as an example of a spherical shaped tumour (Fig. 2).

Motion patterns

The tumour was tracked in the superior-inferior direction based on marker motion, during the breath-hold fluoroscopy acquisitions. The signal was further used to drive the air pressure controlling the inflation of the lungs of the phantom, and thereby the movement of the cylindrical tube containing the tumour. As multiple breath-holds were required to deliver the field, the phantom was set to exhale and inhale between the breath-holds to resemble clinical settings. The beam was gated such to be on during the breath-holds and off in-between, using the Polaris SPECTRA optical tracking system (Northern Digital Inc., Waterloo, CA, USA), which was integrated into the in-house-developed treatment control system [30].

For patient 1, the experiment was repeated with free-breathing motion patterns from the same patient. For the ball case, the breath-hold motion pattern with the largest amplitude (patient 3) was used.

Treatment planning

The planning target volume (PTV) margin was calculated to be 5 mm in anterior-posterior as well as cranio-caudal direction, but 4 mm in left–right direction based on van Herk et al. [31] and clinical data [18]. The PTV volume that received 95% of the prescribed dose (V95%) was always higher than 90%. Prescribed dose was 2 Gy (relative biological efficiency, RBE) to the PTV using RBE = 1.1. The target and OARs were manually segmented in Velocity AI (Varian Medical Systems, Palo Alto, CA, USA). The image intensity of the tumour and holder material was corrected for, according to Supplementary Table S1. SFUD and IMPT treatment plans with three fields each (gantry angles 30°, 250° and 330°) were planned using the in-house treatment planning system at Paul Scherrer Institute (PSI, Villigen, Switzerland) [28]. The couch angle was 10° for the irradiations of transversal films (Patients 2 and 3), and 0° for the other cases. The Hounsfield unit (HU) of the PTV margin was increased to achieve better target coverage ($HU_{margin} = HU_{target}$) for SFUD plans only, and this was verified by recalculation of the

optimised pencil beams on the nominal CT. The dose was normalised to the mean target dose, and for IMPT additionally increased 1–3% for sufficient target coverage.

Experimental setup

The treatment plans were based on static CT scans where the tumour was in an average breath-hold position according to the motion pattern of the individual patient. Since the deformable phantom could be influenced by inherent geometrical deformations between the planning and delivery sessions, CT imaging with 3D-3D matching focusing on soft-tissue to the planning CT was deemed necessary. Furthermore, as the target had to be manually placed within the phantom, its position was subject to set-up errors which was minimised using image guidance. The treatment deliveries under breath-hold conditions were followed by a treatment delivery under complete static conditions as a comparison. An example movie of the phantom LuCa when a breath-hold curve is applied is shown in Supplementary Video S1.

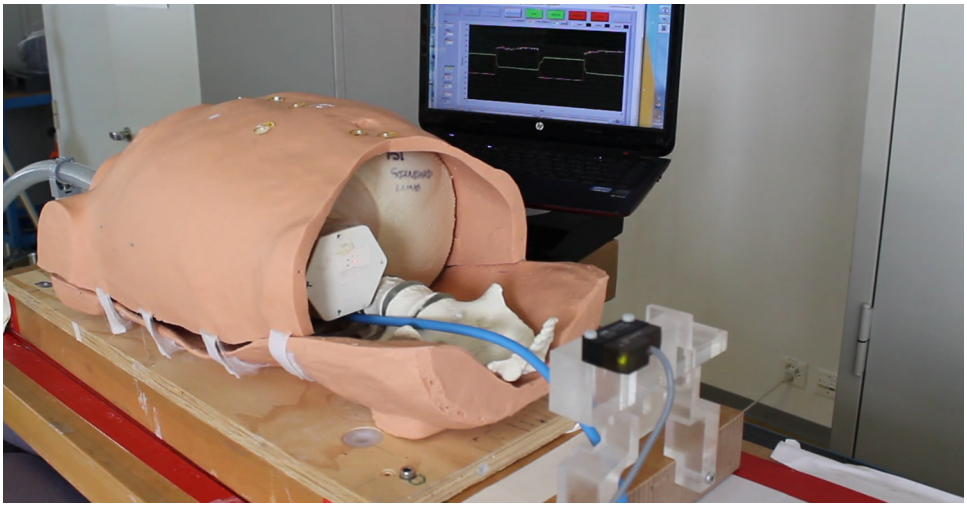

Supplementary Video S1.

In order to bench-mark the reproducibility of the experimental method, repeated measurements with beam gating were carried out for both a breath-hold IMPT (n = 3) and SFUD plan (n = 4). The phantom performed two identical breath-holds during the gated treatment delivery. Intra-breath-hold motion was not allowed for at these repeated set-ups so that exactly identical conditions could be reproduced, allowing for possible beam delays due to interlocks or beamline fluctuations. As a reference for dosimetric comparison the same SFUD and IMPT plans were delivered under a static state, with no beam gating. As in the breath-hold motion investigations, film planes were exchanged between the repeated measurements. The reproducibility was then evaluated in terms of dose difference between static and breath-hold cases.

The target dose was measured using a double layer of radiochromic EBT3 films for which the dose–response curve was characterized [32]. Briefly, measurement of the relative dose–response proceeded as follows. Six iso-energy layer square fields for different doses ranging over the prescribed dose (range: 50–110%) were measured. Squares of film cut from the same sheets used for the phantom measurements were placed at 100 cm source-axis-distance (SAD) in the plateau region of the iso-energy layer (beam energy = 180 MeV), with the nozzle fully extended to match the airgap that was present in the experiments. The average dose to the target from one CT scan was measured and subtracted from the final results, according to the number of CT scans necessary for the setup, to correct for the imaging dose. Furthermore, to reduce the error due to film digitization, each film was scanned three times using a flatbed scanner in transmission mode. The films were scanned before the dose delivery to measure the background transmission over the film plane, for pixel-wise background subtraction.

Analysis

The first analysis included comparison of the motion pattern extracted from the distance sensor during the experiment to the original motion pattern as extracted from the fluoroscopy imaging. Secondly, the digitised films were calibrated in dose, excluding a margin of 3 mm at the edge of the film, due to lack of film integrity in the process of cutting the films into the target-specific shapes. As an absolute dosimetry calibration was not performed, the dose was normalised to the mean dose of the experiment under static conditions, for each case. Dose difference distributions were constructed by pixel-wise subtraction of the dose distributions acquired under breath-hold and static conditions. The mean and standard deviation (square root of the variance) values of all pixels were calculated from these difference distributions for each patient case separately, in addition to the percentage of voxels receiving more than 5% under-dosage. Lastly, gamma pass rate (criteria: 3%, 3 mm) of the breath-hold and static deliveries were computed.

The reproducibility investigation was similarly evaluated. A scale factor for absolute film dose differences had to be applied due to film dose–response differences. This was reasonable as the dose pattern was very similar over the repeated film measurements, leading to a confident conclusion that absolute dose differences were attributable to individual film dose–response differences rather than dose degradation.

Results

Target motion patterns from the original fluoroscopy acquisitions are shown in Fig. 3, together with the target motion patterns as detected by the distance sensor during the experiments. The original motion amplitudes were 3 mm (patient 1), 9 mm (patient 1 free-breathing), and 5 mm (patients 2 and 3). For all cases, the

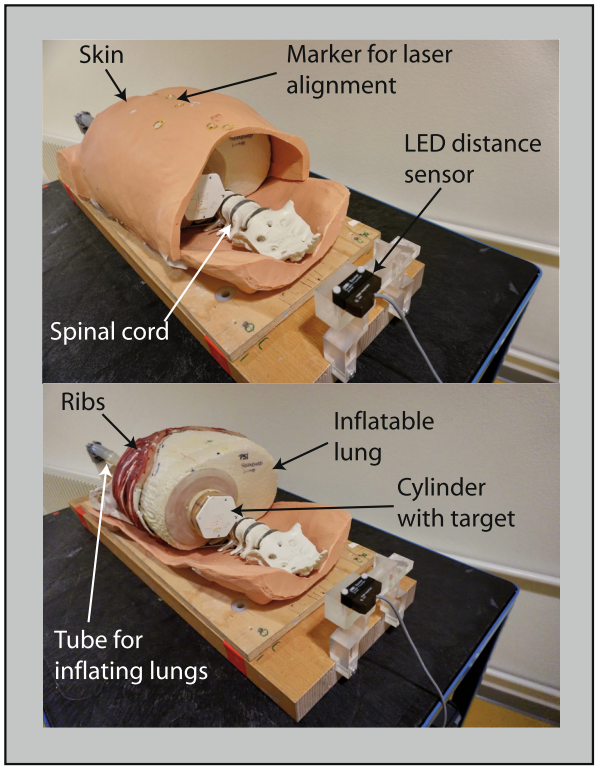

Fig. 1. Photos of the 4D breathing phantom with skin (top) and without skin (bottom).

largest deviation of the experimentally detected target motion in the phantom from the actual patient tumour motion pattern was 2 mm, except for one breath-hold (patient 2) where the error was around 4–5 mm. The free-breathing pattern deviated from the original one by 3 mm or less (peak-to-peak) over the whole delivery, and was faithful to the original pattern shape. Between the planning and experimental session, the motion pattern deviated by less than 2 mm (data not shown). The breath-hold delivery required 1–3 breath-holds per PBS proton therapy field.

Evaluation of the reproducibility experimental series resulted in seven pixel-wise dose difference distributions (three for IMPT, four for SFUD), and the average over the distributions are quoted as mean ± standard deviation: SFUD −0.3 ± 1.8% and IMPT 0.1 ± 3%. Maximum standard deviation in the dose difference distribution was 2.8% and 3.2% for SFUD and IMPT respectively.

Breath-hold SFUD

The mean pixel-wise target dose differences between dose deliveries under static and breath-hold conditions were less than 4% and standard deviations of the dose difference were less than 3.5% (Figs. 4 and 5). Gamma pass rates were 85% or higher and 5% or less of the voxels received under-dosage of more than 5% (Table 1). The results of the spherical ball case were similar to the patient cases, although hot- and cold-regions were observed on the edges in the superior-inferior (motion) direction.

Breath-hold IMPT

The mean pixel-wise target dose differences between dose deliveries under static and breath-hold conditions were less than

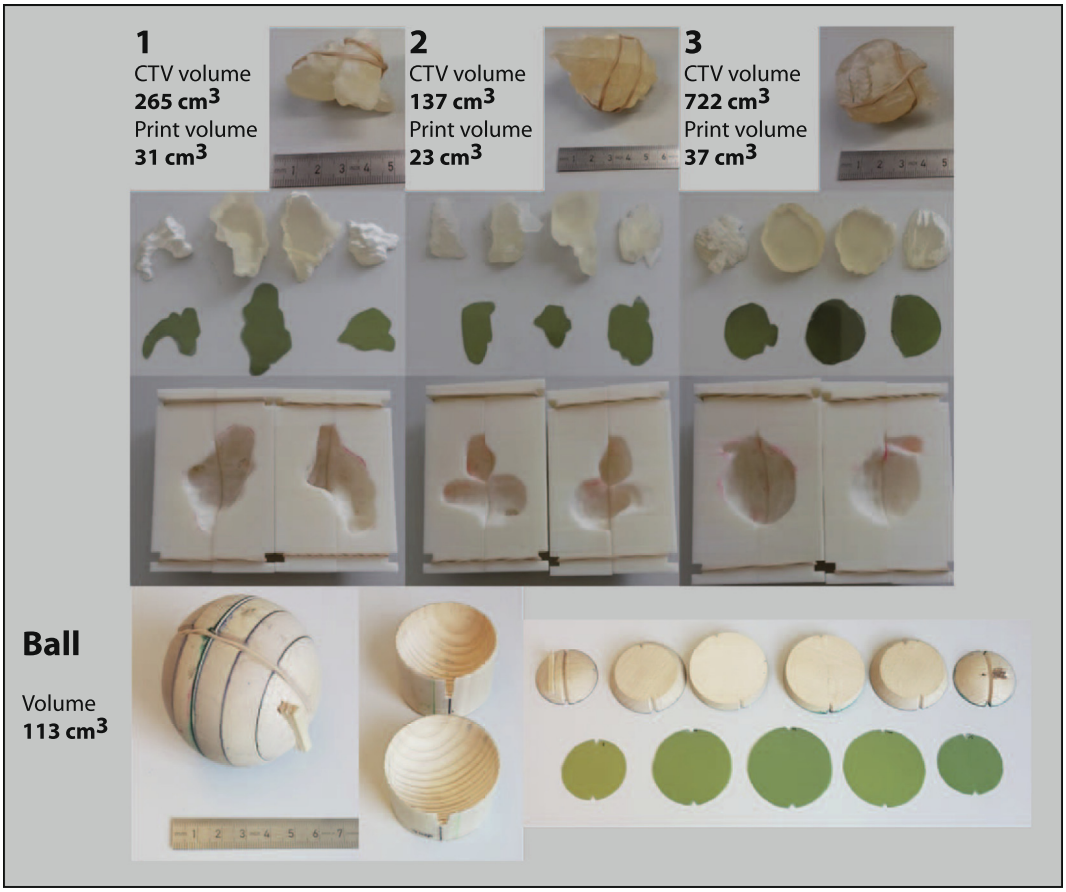

Fig. 2. 3D-printed tumours for patients 1–3 and the wooden ball target together with their holders and radio-chromic films. CTV – clinical target volume.

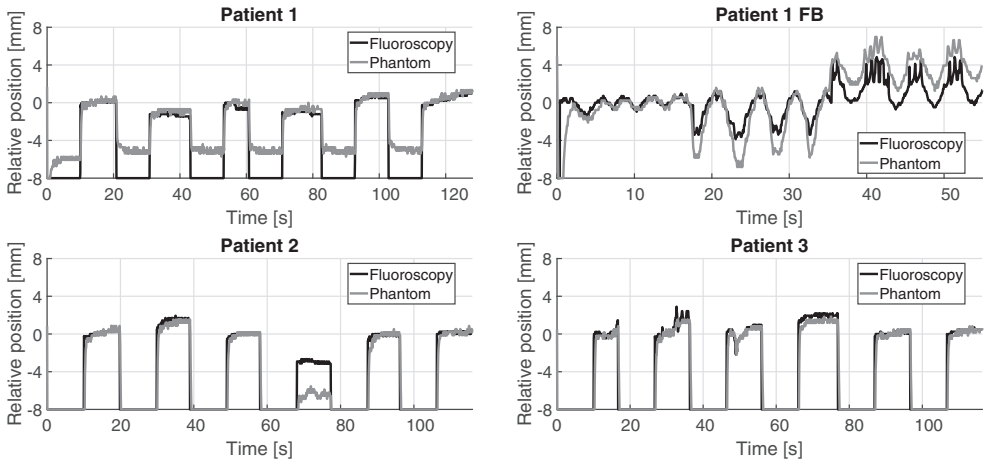

Fig. 3. The motion pattern of the tumour acquired from fluoroscopy and the motion pattern of the target in the phantom measured during the experiment. The exhale was not included in the delivery. FB – free-breathing.

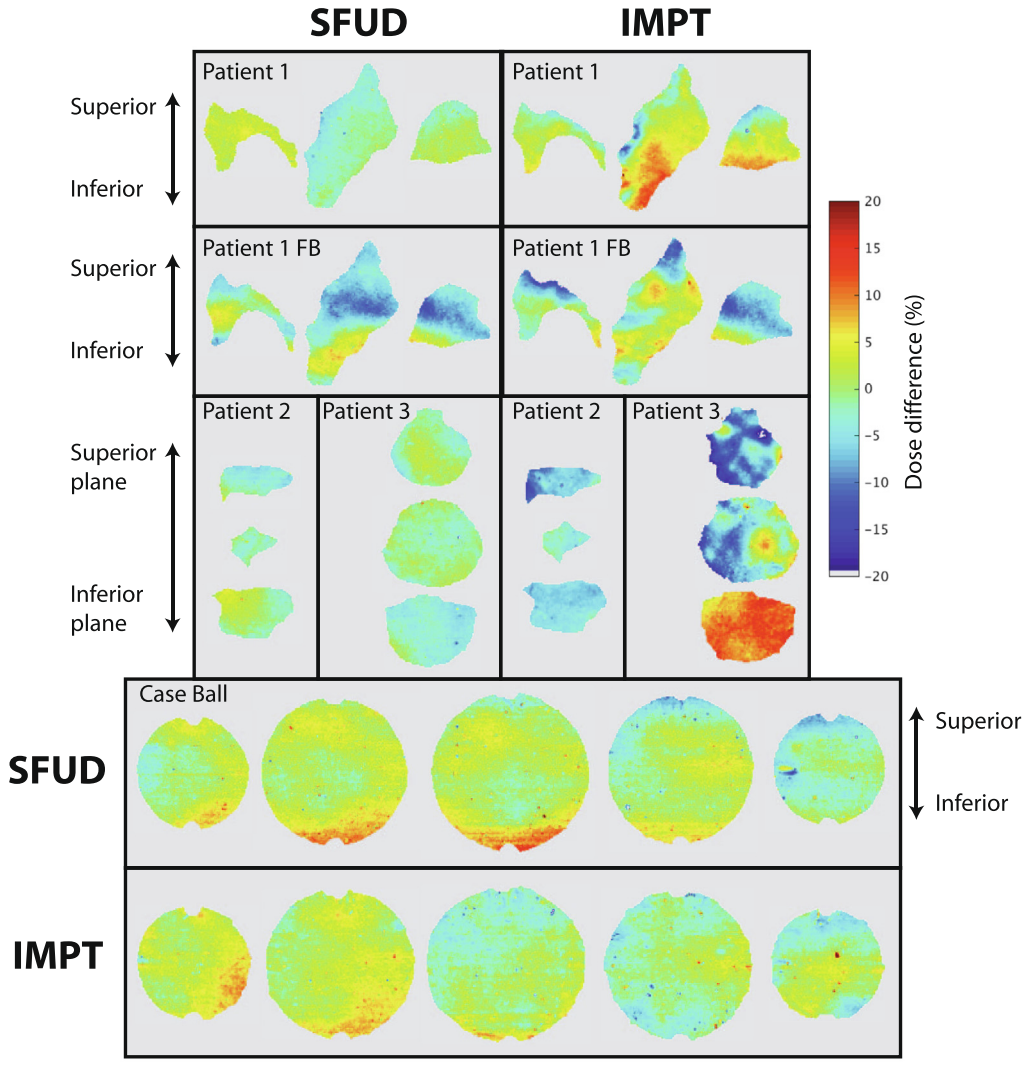

Fig. 4. The difference in terms of breath-hold or free-breathing minus static dose distribution for both single field uniform dose (SFUD) and intensity-modulated proton therapy (IMPT) plans in colour wash according to the legend. Films of patient 1 and Ball were irradiated in the coronal plane and patients 2 and 3 in the transversal plane. The sizes of the film measurements for all cases are true to scale to allow the relative target size to be visualised. FB – free-breathing.

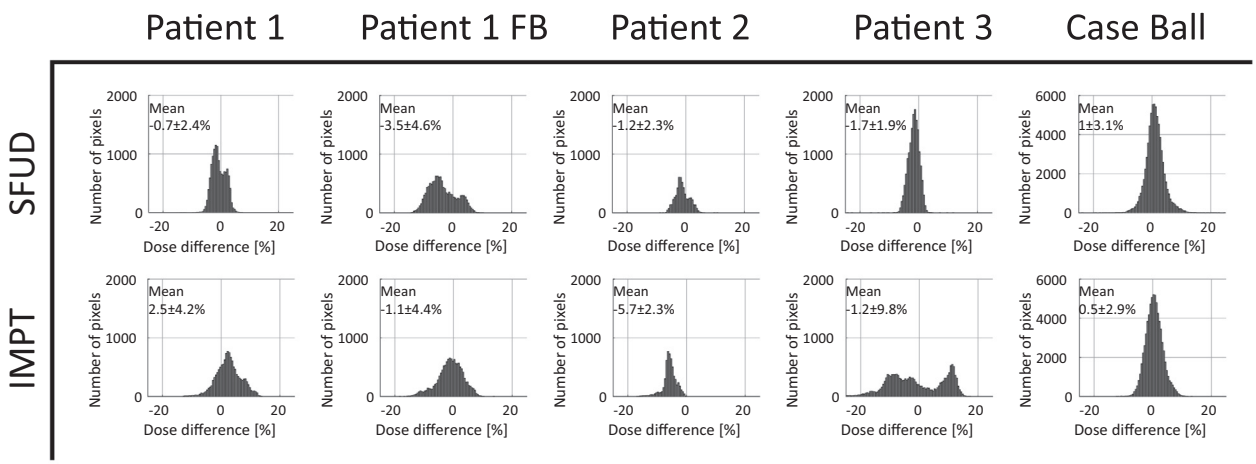

Fig. 5. The histograms of the difference distributions in terms of breath-hold or free-breathing minus static dose distributions for the single field uniform dose (SFUD) and intensity-modulated proton therapy (IMPT) plans. The mean value is given together with the standard deviation. FB – free-breathing.

Table 1
The gamma pass rate and the percentage of voxels with more than 5% under-dosage shown for the single field uniform dose (SFUD) and intensity-modulated proton therapy (IMPT) plans. FB – free-breathing.

Metric	Delivery	Patient 1	Patient 1 FB	Patient 2	Patient 3	Case Ball
Gamma pass rate (3%, 3 mm) [%]	SFUD	95.2	57.5	86.1	90.5	86.1
More than 5% under-dosage [% of voxels]	SFUD	1.7	43.1	4.8	3.9	2.5
Gamma pass rate (3%, 3 mm) [%]	IMPT	67.9	82.2	56.4	48.1	83.5
More than 5% under-dosage [% of voxels]	IMPT	3.6	16.5	65.5	40.1	2.2

6% and standard deviations of the dose difference were less than 10% (Figs. 4 and 5). Gamma pass rates were 50–70% and up to 70% of the voxels received more than 5% under-dosage (Table 1). The dose differences of the spherical ball case were smaller than the patient cases (gamma pass rate: 80% and 5% dose deviation in only 2% of the voxels) (Figs. 4 and 5).

Free-breathing SFUD

The gamma pass rate was 57.5% (Figs. 4 and 5, Table 1), and in over 40% of the pixels an under-dosage of more than 5% was observed. Interplay patterns were visible, consistent with the motion direction (Fig. 4).

Free-breathing IMPT

The gamma pass rate was just over 80% (Figs. 4 and 5, Table 1) and in only around 15% of the pixels, an under-dosage of more than 5% was observed. Evidence of interplay was also visible for this case, in the form of adjacent hot and cold regions (Fig. 4).

Discussion

The dosimetric impact of intra-breath-hold stability has been experimentally measured for clinically relevant targets.

General remarks

PBS treatment plans have previously been shown to be robust with respect to inter-breath-hold residual motion [15], which is substantially larger than the intra-breath-hold motion [17,29,33]. However, as mentioned before, even small motion could cause interplay effects also seen in Fig. 4 for the IMPT breath-hold cases. Rescanning mitigates the effect of small motions (<5 mm) [9,13], but rescanning will inevitably increase the treatment time, which is undesirable for patients with lung disease treated in breath-hold. Another alternative is the use of rescanning in combination with beam gating, which could be more comfortable for the patients. However, beam gating could potentially have larger uncertainties in terms of system latency. In addition, the breath-hold technique has a benefit over beam gating if the entire fraction dose could be delivered in a single breath-hold, as the positional uncertainty between the short dose deliveries would be eliminated. For this, the line scanning delivery technique for PBS has shown promising results regarding substantially shortening the treatment time [34].

The phantom was setup with CT scans using the same lung pressure as for the planning session. Even so, the tumour motion as detected by the distance sensor, varied up to 2 mm from day to day. This is in accordance to the motion reproducibility of the phantom [27]. Online treatment planning, i.e. treatment planning during the treatment/experimental session as discussed in e.g. Oborn et al. [35], could eliminate this source of error of daily variations.

Previously published phantom studies in lung irradiation with proton therapy are small in number, most probably owing to the difficulty in measurement of proton irradiations in a clinically relevant geometry, i.e. including motion, deformation and large density heterogeneities. Steidl et al. [26] demonstrated that a dose degradation is detectable (around 10%) using a complex thorax phantom for a 0.13 mm drift per second, approaching a level comparable to the worst-case intra-breath-hold target drift of ~0.20 mm drift per second in the present study. Another example is Taylor et al. [36] who curated measurements with radio-chromic film and thermoluminescent dosimeters (TLDs) with moving lung and liver phantoms. The dosimetric agreement with planned dose was worse for the moving anthropomorphic phantom as compared with dosimetric agreements measured in static phantoms. This demonstrated the difficulty in end-to-end testing of motion-mitigated treatments with PBS, and also in part to the pencil beam

dose calculation algorithm being inadequate for calculation of proton dose through lung [37]. In light of these reports, our phantom and experimental method, that allows detection of dose degradation of ~3% relative to the reference dose, was entirely reasonable.

A limitation of this study was the use of radio-chromic film as dosimeter. Although the spatial resolution is high, the dose–response is difficult to calibrate since there are numerous sources of errors. Therefore, relative dosimetry was performed comparing static to breath-hold deliveries. Aside from the dosimetric limitation, the films had to be exchanged in between the experiments, adding an additional positional uncertainty. The use of online image-guidance minimised this error (errors in angle of the film plane ±1°, error in positioning ±2 mm). Furthermore, the evaluation of set-up reproducibility at <3% (relative dose difference) added strength to the results of the present study, with dose differences detected over this threshold. This is especially true for the IMPT cases 2 and 3 where an underdosage of >5% was detected in >40% voxels. Finally, the dose was only detected in three or five planes in the tumour, and hence the full 3D dose distribution information was lacking. Future developments are therefore warranted to replace the film dosimetry with a suitable 3D detector, preferably digital for online read-out, avoiding the need to disturb the experimental setup.

Another limitation of this study is the lack of repeated measurements of the breath-hold with intra-fraction motion and a low number of patient tumour cases. A larger number of cases and repeated measurements would strengthen the conclusions from this study. However, the reproducibility of the experimental method was evaluated in separate experiments and demonstrated that the set-up was reproducible and that dose-differences due to motion-related dose degradation >3% could feasibly be detected. The small number of experiments was chosen to enable the measurements to be performed under realistic clinical conditions (highly irregularly-shaped tumours) and intra-breath-hold target drift. This time-consuming experimental setup takes uncertainties including set-up errors, deformable density variations, optical gating uncertainties and motion variations into account. In this light, these measurements have a higher value than a larger amount of measurements under less clinically relevant conditions. In addition, these few cases were of variable size, shape and motion to cover a wide range of clinical scenarios.

SFUD plans in comparison to IMPT plans

For all breath-hold scenarios, dose differences were found to be lower for SFUD than for IMPT plans. The homogeneity in terms of the $D_{5\%}$-$D_{95\%}$ (the dose to 5% or 95% of the volume, respectively) for the individual fields was 20% for SFUD, but over 90% for IMPT (data not shown). Such large inhomogeneities and inter-field dose gradients lead to increased sensitivity to density changes [19] and the conclusion that IMPT plans are more sensitive to motion than SFUD are hence expected and in accordance with previous experience of the proton therapy community. However, this was not so pronounced in the deliveries of the spherical case, perhaps owing to the lower RPSW of the target (0.54), and lower difference in RPSW of the wooden target to the surrounding wood. The latter was rather pronounced in the 3D-printed tumour cases with a ratio of RPSW of the target to surrounding material at around 10 compared to ~2.5 in the spherical wooden ball case. This would produce the effect of larger range changes in the proton spots with respect to target motion drift in the 3D-printed cases, leading to a more marked dose degradation consistent with what was seen in the experiment. There might be several reasons for the differences (or the lack thereof) in results seen between SFUD and IMPT, tumour shape and size being amongst them. In this work however, it has not been possible to distinguish between these. However, a greater robustness to motion for larger target volumes has been previously demonstrated by our group [15]. The effect of irradiating a regular shaped target, as compared to the irregular shaped clinical targets would require further investigations.

SFUD free-breathing

The efficiency of the breath-hold technique as compared to free-breathing was tested in one case and the dosimetric effect of motion was mitigated (gamma pass rates of 95% and 59%, respectively). The extent of under-dosage was substantially reduced using the breath-hold technique.

IMPT free-breathing

Interestingly, the plan delivered under free-breathing as assessed by the gamma pass rate was closer to the static reference than when delivered with breath-hold. This is in contrast to the SFUD plans where the breath-hold technique efficiently mitigated the dosimetric effect of motion as seen in the free-breathing delivery. Even though the gamma pass rate was higher for the IMPT free-breathing than breath-hold delivery, in gamma analysis, both under- and over-dosage are penalised equally. On closer inspection, also for the IMPT case, the extent of under-dose (the most clinically relevant parameter) was indeed found to have been substantially reduced using breath-hold. Nevertheless, this highlights the sensitivity of IMPT to breath-hold gating precision and set-up errors.

Conclusions

SFUD PBS proton therapy plans have in these initial experiments been proven to be robust to the residual intra-breath-hold motion regarding target dose. For IMPT, the dosimetric degradation caused by the motion was more pronounced. Combined motion mitigation strategies (e.g. rescanning) in moving targets treated in breath-hold-mode with IMPT should therefore be considered for further investigations.

Conflict of interest statement

J. Gorgisyan reports funding from Danish Society for Clinical Oncology (DSKO), during the conduct of the study.

This study is part of a PhD dissertation successfully defended at the University of Copenhagen, Denmark. In addition, this study was presented at the 37th annual congress of ESTRO taking place in Barcelona, Spain.

Acknowledgements

The authors would like to thank the Danish Society for Clinical Oncology (DSKO) for funding. The authors would further like to thank Viktor Eggspuehler for the 3D printing.

Appendix A. Supplementary data

Supplementary data to this article can be found online at https://doi.org/10.1016/j.radonc.2019.01.033.

References

[1] Chang JY, Zhang X, Knopf A, Li H, Mori S, Dong L, et al. Consensus guidelines for implementing pencil beam scanning proton therapy for thoracic malignancies on behalf of PTCOG thoracic and lymphoma subcommittee. Int J Radiat Oncol Biol Phys 2017;99:41–50.

[2] Grassberger C, Dowdell S, Sharp G, Paganetti H. Motion mitigation for lung cancer patients treated with active scanning proton therapy. Med Phys 2015;42:2462–9.

[3] Knopf A-C, Stützer K, Richter C, Rucinski A, da Silva J, Phillips J, et al. Required transition from research to clinical application: Report on the 4D treatment planning workshops 2014 and 2015. Phys Med 2016;32:874–82.
[4] Zhang X, Li Y, Pan X, Xiaoqiang L, Mohan R, Komaki R, et al. Intensity-modulated proton therapy reduces the dose to normal tissue compared with intensity-modulated radiation therapy or passive scattering proton therapy and enables individualized radical radiotherapy for extensive stage IIIB non-small-cell lung cancer: a virtual clinical study. Int J Radiat Oncol Biol Phys 2010;77:357–66.
[5] Kamada T, Tsujii H, Blakely EA, Debus J, De Neve W, Durante M, et al. Carbon ion radiotherapy in Japan: an assessment of 20 years of clinical experience. Lancet Oncol 2015;16:e93–e100.
[6] Keall PJ, Mageras GS, Balter JM, Emery RS, Forster KM, Jiang SB, et al. The management of respiratory motion in radiation oncology report of AAPM Task Group 76. Med Phys 2006;33:3874–900.
[7] Underberg RW, Lagerwaard FJ, Slotman BJ, Cuijpers JP, Senan S. Use of maximum intensity projections (MIP) for target volume generation in 4DCT scans for lung cancer. Int J Radiat Oncol Biol Phys 2005;63:253–60.
[8] Knopf A-C, Boye D, Lomax A, Mori S. Adequate margin definition for scanned particle therapy in the incidence of intrafractional motion. Phys Med Biol 2013;58:6079–94.
[9] Jakobi A, Perrin R, Knopf A, Richter C. Feasibility of proton pencil beam scanning treatment of free-breathing lung cancer patients. Acta Oncol 2017:1–8.
[10] Inoue T, Widder J, van Dijk LV, Takegawa H, Koizumi M, Takashina M, et al. limited impact of setup and range uncertainties, breathing motion, and interplay effects in robustly optimized intensity modulated proton therapy for stage III non-small cell lung cancer. Int J Radiat Oncol Biol Phys 2016;96:661–9.
[11] Bernatowicz K, Zhang Y, Perrin R, Weber DC, Lomax AJ. Advanced treatment planning using direct 4D optimisation for pencil-beam scanned particle therapy. Phys Med Biol 2017;62:6595–609.
[12] Eley JG, Newhauser WD, Richter D, Lüchtenborg R, Saito N, Bert C. Robustness of target dose coverage to motion uncertainties for scanned carbon ion beam tracking therapy of moving tumors. Phys Med Biol 2015;60:1717–40.
[13] Zenklusen SM, Pedroni E, Meer D. A study on repainting strategies for treating moderately moving targets with proton pencil beam scanning at the new Gantry 2 at PSI. Phys Med Biol 2010;55:5103–21.
[14] Mori S, Wolfgang J, Lu H-M, Schneider R, Choi NC, Chen GTY. Quantitative assessment of range fluctuations in charged particle lung irradiation. Int J Radiat Oncol Biol Phys 2008;70:253–61.
[15] Dueck J, Knopf A-C, Lomax A, Albertini F, Persson GF, Josipovic M, et al. Robustness of the voluntary breath-hold approach for the treatment of peripheral lung tumors using hypofractionated pencil beam scanning proton therapy. Int J Radiat Oncol Biol Phys 2016;95:534–41.
[16] Kanehira T, Matsuura T, Takao S, Matsuzaki Y, Fujii Y, Fujii T, et al. Impact of real-time image gating on spot scanning proton therapy for lung tumors: a simulation study. Int J Radiat Oncol Biol Phys 2017;97:173–81.
[17] Hanley J, Debois MM, Mah D, Mageras GS, Raben A, Rosenzweig K, et al. Deep inspiration breath-hold technique for lung tumors: the potential value of target immobilization and reduced lung density in dose escalation. Int J Radiat Oncol Biol Phys 1999;45:603–11.
[18] Josipovic M, Persson GF, Dueck J, Bangsgaard JP, Westman G, Specht L, et al. Geometric uncertainties in voluntary deep inspiration breath hold radiotherapy for locally advanced lung cancer. Radiother Oncol 2016;118:510–4.
[19] Stuschke M, Kaiser A, Pöttgen C, Lübcke W, Farr J. Potentials of robust intensity modulated scanning proton plans for locally advanced lung cancer in comparison to intensity modulated photon plans. Radiother Oncol 2012;104:45–51.
[20] Knopf A-C, Hong TS, Lomax A. Scanned proton radiotherapy for mobile targets—the effectiveness of re-scanning in the context of different treatment planning approaches and for different motion characteristics. Phys Med Biol 2011;56:7257.
[21] Phillips MH, Pedroni E, Blattmann H, Boehringer T, Coray A, Scheib S. Effects of respiratory motion on dose uniformity with a charged particle scanning method. Phys Med Biol 1992;37:223.
[22] Persson GF, Josipovic M, von der Recke P, Aznar MC, Juhler-Nøttrup T, Munck af Rosenschöld P, et al. Stability of percutaneously implanted markers for lung stereotactic radiotherapy. J Appl Clin Med Phys 2013;14:187–95.
[23] Meijer GJ, van der Toorn P-P, Bal M, Schuring D, Weterings J, de Wildt M. High precision bladder cancer irradiation by integrating a library planning procedure of 6 prospectively generated SIB IMRT plans with image guidance using lipiodol markers. Radiother Oncol 2012;105:174–9.
[24] Scherman Rydhög J, Irming Jølck R, Andresen TL, Munck af Rosenschöld P. Quantification and comparison of visibility and image artifacts of a new liquid fiducial marker in a lung phantom for image-guided radiation therapy. Med Phys 2015;42:2818–26.
[25] Koybasi O, Mishra P, St James S, Lewis JH, Seco J. Simulation of dosimetric consequences of 4D-CT-based motion margin estimation for proton radiotherapy using patient tumor motion data. Phys Med Biol 2014;59:853–67.
[26] Steidl P, Richter D, Schuy C, Schubert E, Haberer T, Durante M, et al. A breathing thorax phantom with independently programmable 6D tumour motion for dosimetric measurements in radiation therapy. Phys Med Biol 2012;57:2235–50.
[27] Perrin RL, Zakova M, Peroni M, Bernatowicz K, Bikis C, Knopf A, et al. An anthropomorphic breathing phantom of the thorax for testing new motion mitigation techniques for pencil beam scanning proton therapy. Phys Med Biol 2017;62:2486–504.
[28] Lomax AJ, Böhringer T, Bolsi A, Coray D, Emert F, Goitein G, et al. Treatment planning and verification of proton therapy using spot scanning: initial experiences. Med Phys 2004;31:3150–7.
[29] Rydhög JS, de Blanck SR, Josipovic M, Jølck RI, Larsen KR, Clementsen P, et al. Target position uncertainty during visually guided deep-inspiration breath-hold radiotherapy in locally advanced lung cancer. Radiother Oncol 2017;123:78–84.
[30] Fattori G, Safai S, Carmona PF, Peroni M, Perrin R, Weber DC, et al. Monitoring of breathing motion in image-guided PBS proton therapy: comparative analysis of optical and electromagnetic technologies. Radiat Oncol 2017;12:63.
[31] van Herk M, Remeijer P, Rasch C, Lebesque JV. The probability of correct target dosage: dose-population histograms for deriving treatment margins in radiotherapy. Int J Radiat Oncol Biol Phys 2000;47:1121–35.
[32] Reinhardt S, Hillbrand M, Wilkens JJ, Assmann W. Comparison of Gafchromic EBT2 and EBT3 films for clinical photon and proton beams. Med Phys 2012;39:5257–62.
[33] Garibaldi C, Catalano G, Baroni G, Tagaste B, Riboldi M, Spadea MF, et al. Deep inspiration breath-hold technique guided by an opto-electronic system for extracranial stereotactic treatments. J Appl Clin Med Phys 2013;14:14–25.
[34] Schätti A, Meer D, Lomax AJ. First experimental results of motion mitigation by continuous line scanning of protons. Phys Med Biol 2014;59:5707–23.
[35] Oborn BM, Dowdell S, Metcalfe PE, Crozier S, Mohan R, Keall PJ. Future of medical physics: real-time MRI-guided proton therapy. Med Phys 2017;44:e77–90.
[36] Taylor PA, Kry SF, Alvarez P, Keith T, Lujano C, Hernandez N, et al. Results from the Imaging and radiation oncology core Houston's anthropomorphic phantoms used for proton therapy clinical trial credentialing. Int J Radiat Oncol Biol Phys 2016;95:242–8.
[37] Taylor PA, Kry SF, Followill DS. Pencil beam algorithms are unsuitable for proton dose calculations in lung. Int J Radiat Oncol Biol Phys 2017;99:750–6.